

Carrier-induced fast wavelength switching in tunable V-cavity laser with quantum well intermixed tuning section

Xin Zhang,¹ Jian-Jun He,^{1,*} Neng Liu,² and Jan J. Dubowski²

¹Centre for Integrated Optoelectronics, State Key Laboratory of Modern Optical Instrumentation, Zhejiang University, Hangzhou, 310027, China

²Interdisciplinary Institute for Technological Innovation (3IT), Department of Electrical and Computer Engineering, Université de Sherbrooke, 3000 boul. de l'Université, Sherbrooke, Québec J1K 0A5, Canada
[*jjhe@zju.edu.cn](mailto:jjhe@zju.edu.cn)

Abstract: We report on the fast wavelength switching in V-cavity laser (VCL) with quantum well intermixed tuning section. The laser wavelength can be switched between 32 channels at 100 GHz spacing using a single electrode control. The fabrication process involves a quantum well intermixing (QWI) process using KrF laser irradiation and rapid thermal annealing (RTA). The tuning current is less than 40 mA, much lower than previously demonstrated tunable VCL based on electro-thermal-optic effect. The wavelength switching is also faster by three orders of magnitude. The dynamic switching characteristics between two channels with different numbers of intermediate channels are investigated. It shows that the switching time is about 1 ns between adjacent channels and increases up to 12 ns with increasing number of intermediate channels.

©2015 Optical Society of America

OCIS codes: (140.5960) Semiconductor lasers; (250.5300) Photonic integrated circuits.

References and links

1. L. Coldren, "Monolithic tunable diode lasers," *IEEE J. Sel. Top. Quantum Electron.* **6**(6), 988–999 (2000).
 2. J.-J. He and D. Liu, "Wavelength switchable semiconductor laser using half-wave V-coupled cavities," *Opt. Express* **16**(6), 3896–3911 (2008).
 3. J. Jin, L. Wang, T. Yu, Y. Wang, and J.-J. He, "Widely wavelength switchable V-coupled-cavity semiconductor laser with ~40 dB side-mode suppression ratio," *Opt. Lett.* **36**(21), 4230–4232 (2011).
 4. S. Zhang, J. Meng, S. Guo, L. Wang, and J.-J. He, "Simple and compact V-cavity semiconductor laser with 50×100 GHz wavelength tuning," *Opt. Express* **21**(11), 13564–13571 (2013).
 5. S. Guo, J. Meng, L. Wang, L. Zou, H. Zhu, and J.-J. He, "Experimental demonstration of subnano-second wavelength switching in V-coupled-cavity semiconductor laser," in *Asia Communications and Photonics conference* (2012).
 6. W. D. Laidig, N. Holonyak, Jr., M. D. Camras, K. Hess, J. J. Coleman, P. D. Dapkus, and J. Bardeen, "Disordering of an AlAs-GaAs superlattice by impurity diffusion," *Appl. Phys. Lett.* **38**(10), 776–778 (1981).
 7. B. S. Ooi, K. McIlvaney, M. W. Street, A. S. Helmy, S. G. Ayling, A. C. Bryce, J. H. Marsh, and J. Roberts, "Selective quantum-well intermixing in GaAs-AlGaAs structures using impurity-free vacancy diffusion," *IEEE J. Quantum Electron.* **33**(10), 1784–1793 (1997).
 8. H. Djie, T. Mei, J. Arokiaraj, C. Sookdhis, S. Yu, L. Ang, and X. Tang, "Experimental and theoretical analysis of argon plasma-enhanced quantum-well intermixing," *IEEE J. Quantum Electron.* **40**(2), 166–174 (2004).
 9. S. Charbonneau, E. S. Koteles, P. Poole, J.-J. He, G. Aers, J. Haysom, M. Buchanan, Y. Feng, A. Delage, F. Yang, M. Davies, R. D. Goldberg, P. G. Piva, and I. V. Mitchell, "Photonic integrated circuits fabricated using ion implantation," *IEEE J. Sel. Top. Quantum Electron.* **4**(4), 772–793 (1998).
 10. S. D. McDougall, O. P. Kowalski, C. J. Hamilton, F. Camacho, B. Qiu, M. Ke, R. M. De La Rue, A. C. Bryce, and J. H. Marsh, "Monolithic integration via a universal damage enhanced quantum-well intermixing technique," *IEEE J. Sel. Top. Quantum Electron.* **4**(4), 636–646 (1998).
 11. M. Kaleem, X. Zhang, Y. Zhuang, J.-J. He, N. Liu, and J. J. Dubowski, "UV laser induced selective-area bandgap engineering for fabrication of InGaAsP/InP laser devices," *Opt. Laser Technol.* **51**, 36–42 (2013).
 12. R. Beal, V. Aimez, and J. J. Dubowski, "Excimer laser induced quantum well intermixing: a reproducibility study of the process for fabrication of photonic integrated devices," *Opt. Express* **23**(2), 1073–1080 (2015).
 13. E. J. Skogen, J. S. Barton, S. P. DenBaars, and L. A. Coldren, "Tunable sampled-grating DBR lasers using quantum-well intermixing," *IEEE Photonics Technol. Lett.* **14**(9), 1243–1245 (2002).
-

14. E. J. Skogen, J. W. Raring, J. S. Barton, S. P. Denbaars, and L. A. Coldren, "Postgrowth control of the quantum-well band edge for the monolithic integration of widely tunable lasers and electroabsorption modulators," *IEEE J. Sel. Top. Quantum Electron.* **9**(5), 1183–1190 (2003).
 15. S. J. Pearton, A. Katz, and M. Geva, "Reproducible group-V partial pressure rapid thermal annealing of InP and GaAs," *J. Appl. Phys.* **68**(5), 2482–2488 (1990).
 16. O. Hulko, D. A. Thompson, J. A. Czaban, and J. G. Simmons, "The effect of different proximity caps on quantum well intermixing in InGaAsP/InP QW structures," *Semicond. Sci. Technol.* **21**(7), 870–875 (2006).
-

1. Introduction

Widely tunable lasers that are capable of tuning to any channel on the international telecommunication union (ITU) grid will dramatically reduce the cost of the optical telecommunication systems [1]. V-cavity laser (VCL) is a promising tunable laser solution for low-cost access networks, due to its compactness and fabrication simplicity [2–4]. However, all the VCL reported so far adopted heat-induced wavelength tuning, leading to high driving current (>120 mA) and low wavelength switching speed (>10 μ s). By applying the carrier-induced wavelength tuning, the driving current was much lower, and the wavelength switching time was at the nanosecond level [5]. To achieve the large-range carrier tuning effect, the tuning waveguide section is required to be passive to avoid the carrier clamping effect. One of the most simple and promising techniques for active-passive integration is quantum well intermixing (QWI). In this technique, point defects are firstly generated on the surface of the sample. These defects then diffuse into the quantum well (QW) layers during a rapid thermal annealing (RTA) process, leading to the intermixing of barrier and well of the QW layers. There are many QWI techniques reported in the past decades, such as impurity induced disordering (IID) [6], impurity free vacancy disordering (IFVD) [7], argon plasma induced disordering [8], ion implantation induced disordering (IIID) [9] and SiO₂ sputtering induced disordering [10]. However, most of these techniques lack the reproducibility and the reliability required for industrial fabrication. KrF laser irradiation based QWI is recently reported to be potentially attractive due to its high reproducibility and reliability [11,12]. We used this technique to selectively modify the QW energy band gap in the tuning waveguide sections.

Ion implantation induced QWI has been used for active-passive integration in sampled grating distributed Bragg reflector (SGDBR) tunable lasers [13,14]. In this paper, we report the first experimental results of carrier-induced wavelength tuning in VCL with quantum well intermixed tuning section. The single-electrode control of wavelength switching in VCL is particularly important for realizing fast switching employing the carrier plasma effect as compared to multi-electrode controlled tunable lasers such as SG-DBR based lasers. 32-channel wavelength tuning at 100 GHz spacing with single-electrode control is demonstrated, and the side mode suppression ratio (SMSR) reaches 35 dB. The wavelength switching time between two channels with different intermediate channel numbers are investigated.

2. Device design and fabrication

Figure 1 shows the top-view photograph of the VCL. It contains two cavities with different lengths. The length of the short cavity is designed so that its resonant wavelengths match the ITU grids of 100 GHz spacing. The other cavity is 5% longer, so that the wavelength tuning range is magnified by the Vernier effect. The coupler that combines the two cavities is a specially designed half-wave coupler, which raises the SMSR to over 40 dB theoretically. The three deep-etched facets are used to accurately control the lengths of the cavities and the coupler. The waveguides under the long and short cavity electrodes are processed to be passive waveguides using QWI technology. In operation, a fixed current is applied to the gain electrode. A tuning current on the long cavity electrode changes the effective refractive index of the waveguide underneath based on the carrier injection effect, so that the wavelength of the laser is tuned. Theoretically, the tuning range is limited by the free spectral range (FSR) of the Vernier effect (around 20 channels for 5% cavity length differences).

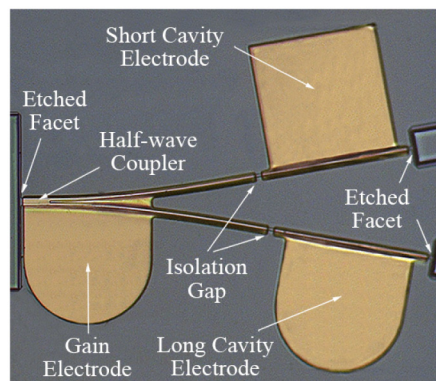


Fig. 1. Schematic structure of the VCL.

The sample is a 1.2% compressive strained laser structure containing five InGaAsP QWs with InGaAsP barriers, with the emission wavelength around 1.55 μm . From the surface the layers contain a 0.5 μm Zn-doped InP sacrificial layer, 0.2 μm Zn-doped $\text{In}_{0.53}\text{Ga}_{0.47}\text{As}$ cap, 1.5 μm Zn-doped InP cladding, 0.004 μm InGaAsP etch-stop layer, five InGaAsP QWs which are sandwiched by two 0.06 μm InGaAsP step-graded index confining layers, and Si-doped InP buffer on Si-doped InP substrate.

For the device fabrication, alignment marks were first etched into the upper cladding layer by the standard photolithography and dry etching process followed by KrF laser based QWI process carried out in selected regions. Finally, a standard VCL fabrication procedure was executed.

During the KrF laser based QWI process, a series of SiO_2 windows with the size of 200 $\mu\text{m} \times 200 \mu\text{m}$ and the thickness of 200 nm were firstly made with photolithography and dry etching process. Then a KrF laser beam (ProMaster OPTEC, ATLEX 300i, $\lambda = 248 \text{ nm}$) with the spot size of 40 $\mu\text{m} \times 40 \mu\text{m}$ scanned all the regions inside of these windows at an intensity of 50 J/cm^2 for 50 pulses. After the SiO_2 mask was removed, an RTA process was executed at 750 $^\circ\text{C}$ for 90 s in a flowing nitrogen atmosphere. During the RTA process, the sample was placed between two pieces of Si substrates, which were used to minimize the out-diffusion of P atoms from the surface during the high-temperature annealing [15,16].

3. Measurement results and discussions

When the KrF laser based QWI process was completed, the sample was tested in a photoluminescence (PL) platform. Figure 2(a) shows the PL wavelength map of one QWI window. The PL wavelength outside of the QWI window is around 1530 nm, and 1425 nm inside the window. The net blue shift is therefore around 105 nm. The wavelengths are very uniform both inside and outside of the window, indicating this technique has very good uniformity. The wavelengths at the boundary of this window also change rapidly, showing a great spatial resolution property. Figure 2(b) shows the PL spectra in RTA-only and QWI regions. After KrF laser based QWI process, the net wavelength blue shift is around 105 nm, and peak intensity increases by 20%. The increase of PL intensity indicates that the quality of QW gets even better after KrF laser based QWI process.

For the characterization, the lasers were mounted on a thermo-electric controller (TEC) at 20 $^\circ\text{C}$. The output light was collected from the cleaved facet near the coupler with a multimode fiber. A fixed current was injected on the coupler at 120 mA and a tunable current was injected on the long cavity electrode. As the short cavity was processed to be passive cavity, no current was applied on this electrode.

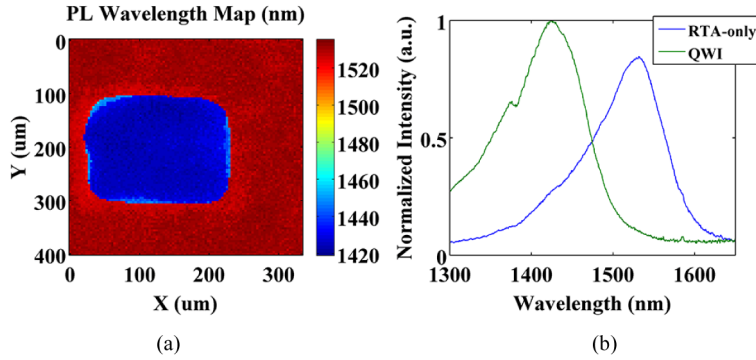


Fig. 2. PL wavelength map (a) and spectra in RTA-only (blue line) and QWI (green line) regions (b) of the KrF laser based QWI sample.

Figure 3 shows the peak wavelength of the VCL when the tuning current was varied from 0 to 40 mA. This tuning current is much lower than that of all active VCL. According to the Vernier effect, when the tuning current is injected into the long cavity of VCL, the carrier injection effect shifts the lasing channel to a shorter wavelength while the thermal effect drives the lasing channel in the opposite direction. As we can see in Fig. 3, the lasing channels move towards shorter wavelength by increasing the tuning current on the long cavity from 0 to 40 mA. This indicates the refractive index decreases with increasing tuning current due to the increasing injecting carrier. As the tuning current further increases, the carrier injection effect tends to saturate and the thermal effect starts to play a dominant role which prevents the channels going further to shorter wavelength.

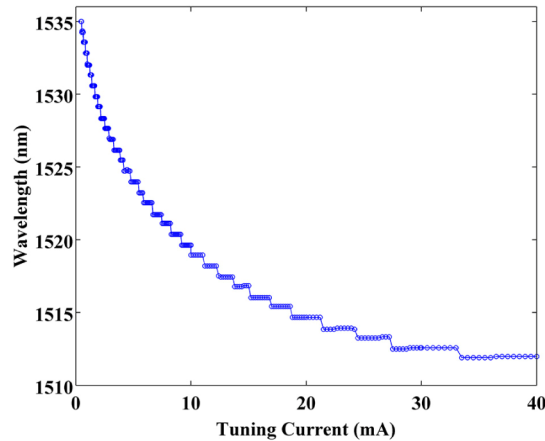


Fig. 3. Tested peak wavelength tuning of VCL.

Figure 4(a) shows the spectra of the 32 channels. The 32 channels are in the range from 1535.0 nm to 1511.8 nm with 100 GHz spacing, and the output light power detected by using a multimode fiber is about 1 mW. The SMSR of each spectrum reach 35 dB as shown in Fig. 4(b). It is comparable to that of all active VCL. This result means the KrF laser based QWI process does not affect the single-mode performance of the laser.

The 32-channel tuning range exceeded the free spectral range of the VCL with 5% cavity length difference, which is only 20 channels. To explain the extra 12 channels, the electroluminescence (EL) spectra were measured from the deep-etched facet near the long cavity electrode. When only the long cavity electrode was injected current, the EL peak wavelength was about 1430 nm, which is almost the same as the PL peak wavelength of QWI window in Fig. 2. When current was only injected into the gain electrode on the coupler, the

EL peak wavelength was around 1535 nm, near the PL wavelength of the RTA-only region. When the current on the long cavity electrode was increased from 0 to 40 mA, the peak wavelength of the EL spectrum was blue shifted from 1535 nm to around 1510 nm. This can be explained by the fact that the shorter wavelength side of the coupler EL was absorbed by the quantum well intermixed waveguide in the tuning section when there was no current injected. When the current in the tuning section increases, the absorption at the shorter wavelength decreases, resulting in a blue shift of the EL. The same effect happens to the average gain spectrum in the cavity. This blue shift of the gain spectrum can be utilized to tune the wavelength beyond the limit of the FSR, since the lasing wavelength is tuned in the same direction by the carrier injection effect through the long cavity electrode. Therefore, the laser channel can go on being tuned to a shorter wavelength until the carrier-induced tuning and heat-induced tuning reach a balance.

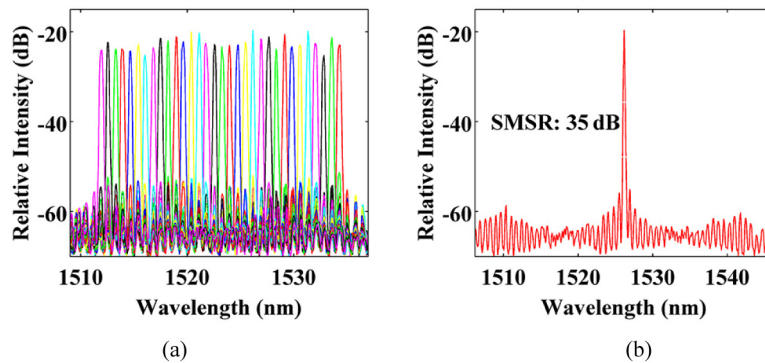


Fig. 4. Tested superimposed 32-channel spectra (a) and single spectrum with SMSR of 35 dB (b) of VCL.

The wavelength switching speed of the laser was measured with optical filter method. A square wave signal (frequency = 155 MHz, duty cycle = 0.5, rise/fall time $T_0 = 700$ ps) was applied to the long cavity electrode, switching the wavelength between two channels. After amplification by an erbium-doped fiber amplifier (EDFA), the light passes through a tunable filter to achieve the wavelength-intensity conversion. Finally, the signal was acquired in an oscilloscope connected at the photo-detector output. Figure 5(a) shows the wavelength switching waveforms between two adjacent channels. The switching time between these two channels are 1.8 ns and 1.7 ns, respectively. Considering the 700 ps of the rise/fall time of the square wave signal, both of the switching times are around 1 ns. This result confirms that the switching mechanism is dominated by the carrier plasma effect. The switching time from the lower current mode (1535 nm) to the higher current mode (1534.2 nm) is a little shorter than that of the opposite direction. This can be explained as the carrier density falls slightly slower than it rises. Figure 5(b) shows the wavelength switching transients between two non-adjacent channels 1532.6 nm and 1535 nm, with 2 intermediate channels 1533.4 nm and 1534.2 nm in between. In this case, signals of intermediate channels appear during the transitions, with the strongest signal from the channel closest to the destination channel, i.e. 1534.2 nm signal when the wavelength is switched from 1532.6 nm to 1535 nm, and 1533.4 nm signal when the wavelength is switched from 1535 nm to 1532.6 nm. The switching times were measured to be 6.6 ns and 6.3 ns, respectively.

The switching time generally increases with the number of intermediate channels. Figure 6 shows the wavelength switching time between two channels as a function of the number of intermediate channels. As the intermediate channel number increases from 0 to 10, the switching time also increases almost linearly from about 1 ns to about 10 ns. However, the increase of the switching time saturates when the intermediate channel number is beyond 11. This can be explained by the fact that the carrier density responds faster to the switching

current pulse at a high current. The switching time is over 3 orders of magnitude faster than that based on electro-thermal-optical effect ($\sim 20\mu\text{s}$) without using QWI [4].

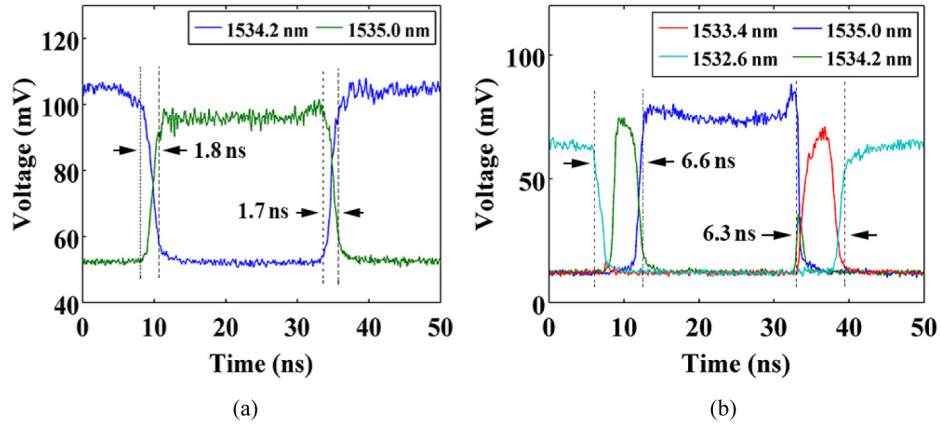


Fig. 5. Wavelength switching waveforms of two consecutive super-modes (a) and super-modes with different intermediate mode number (b)

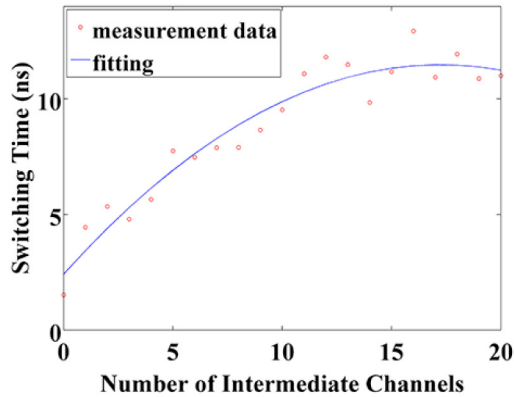


Fig. 6. Wavelength switching time versus the number of intermediate channels.

4. Conclusion

In conclusion, we have designed and fabricated a VCL with carrier-induced wavelength tuning effect using KrF laser based QWI technology. Carrier-induced wavelength tuning of 32 channels at 100 GHz spacing with single electrode tuning was demonstrated. The SMSR was as high as 35 dB. The tuning current was only less than 40 mA. The dynamic wavelength switching characteristics between two channels with different intermediate channel numbers are investigated. The switching time is about 1 ns for two adjacent channels, and increases to up to 12 ns for non-adjacent channels. We believe that the single-electrode controlled fast wavelength switching is very promising for future wavelength routed optical networks.

Acknowledgment

This work is supported by the National High-Tech R&D Program of China (Grant no. 2013AA014401), and the National Science and Technology Major Project of the Ministry of Science and Technology of China (No. 2015ZX03001021).